

Tsunami Modelling and Risk Assessment of Hambantota, Sri Lanka Using Integrated Remote Sensing Techniques

WAM Fernando¹, MLM Aswer¹, MWVS Premarathna¹, M Suthakar¹
DMDOK Dissanayake^{1*}, IP Senanayake¹ and S Samansiri²

¹*Department of Earth Resources Engineering, University of Moratuwa, Sri Lanka*

²*Disaster Management Centre, Sri Lanka*

*Corresponding author: dmdok@uom.lk

Abstract: This study was carried out to develop an inundation and risk assessment model in Hambantota coastal area, based on the 2004 tsunami event. This tsunami event was one of the largest tsunamis to cause devastation to human beings, livelihoods, buildings, roads, rails and other infrastructure facilities in the study area. In addition to this study area, other parts of the coastal belt of Sri Lanka also experienced the chaotic outcomes of this tsunami event. By modelling risk, based on the 2004 tsunami event data, inundation and risk assessment for future tsunami event was modelled with a high safety factor. INSPIRE web portal which has been developed based on the TUNAMI mathematical model, was employed in this study to evaluate both inundation and risks to the local communities and their livelihoods with a higher level of accuracy. The main inputs to INSPIRE are topography data/bathymetry data, vulnerability data and fault parameters of the source earthquake, whereas the output maps provide the inundation area, wave velocity along the terrain and the potential risk to the area under consideration. Results of the study represent the variation of the tsunami inundation and the risk assessment of the Hambantota area based on remotely sensed digital elevation data inputs with different spatial resolutions data such as, ASTER, SRTM, LiDAR and GEBCO. Different inundation output maps were analyzed and the risk prone areas were identified. Furthermore, building structures were assigned risk indices based on the vulnerability to damage and fragility curves were developed in the case of a future tsunami event.

Key Words: Hazard identification, inundation mapping, INSPIRE web portal, numerical simulation, risk assessment, tsunami

1. Introduction

A tsunami is caused by the perturbation of the sea by means of an earthquake, submarine landslides, volcanic eruptions or meteoric impacts. However, from the aforementioned governing factors, 90% of the tsunamis around the world have occurred due to earthquakes (Wong and Chan, 2006). Violent tsunamis as such are capable of destroying both human lives and property which can easily push a country's development backwards. The Boxing Day tsunami in 2004 has earned the top position of the 'Largest death tolls from tsunamis over the last 2000 years' list and the 5th place of the 'Deadliest natural disasters since 1900' list (Berger, 2010; Bryant, 2008). Eliminating risks is not always easy due to the unpredictable nature of the natural phenomena. Hence, the key to successfully survive a natural hazard such as a tsunami is to reduce the risks that it might impose on a specific area. The real challenge of reducing the risks of a tsunami is to predict the extent of inundation of such an event. Once the extent is clearly distinguished, the loss of lives and property can be easily minimized. This study concentrates on hazard and risk mapping of Hambantota area of Sri Lanka which was severely affected by the 2004 tsunami.

2. Objectives of the study

The overall aim of the study was to introduce a feasible tsunami modelling method using the INSPIRE

web portal to reduce the damage on both human lives and property. The pathway to that ultimate goal, the following objectives have to be fulfilled.

- Estimate the inundation area caused by a tsunami within the Hambantota city.
- Identification of tsunami risk prone areas and building structures.
- Identification of the most cost effective way to collect data for tsunami modelling.
- Development of fragility curves for a specific building type in Hambantota area.

3. Methodology

The methodology of this study was based on the INSPIRE web portal. The TUNAMI computational tool was employed in this study to evaluate tsunami inundation and risk mapping. The TUNAMI computational tool is given a graphical interface by the INSPIRE web portal developed by Regional Integrated Multi-Hazard Early Warning System (RIMES). INSPIRE web portal is capable of generating outcomes such as tsunami inundation modelling, velocity of the tsunami waves, tsunami risk prone areas and the assessment of the risks.

3.1 Data and Materials

To perform the simulation, INSPIRE requires four Digital Elevation Model (DEM) files & deformation

parameters of the earthquake. For DEM preparation four datasets were employed in this study by dividing the area from the earthquake epicentre to the area of interest into four regions (Figure 3.1).



Figure 3.1: Four regions defined for the tsunami simulation

Three of the four required files were bathymetric (i.e. GEBCO 2 arc minute, 15 arc second, 5 arc second) data of the ocean and the fourth one was a topographic dataset. Three datasets of the area in concern, with different spatial resolutions namely LiDAR (5m), SRTM (90m) and ASTER (30m) were uploaded separately for each simulation. The four regions were defined in accordance to the longitudes and the latitudes. The spatial resolution of the four regions increase from region 1 to region 4 where region 1 covers the largest area and region 4 covers the area under consideration. For the simulation to initiate, the initial deformation surface has to be defined. In this study, the initial deformation surface was divided into 6 segments and the

parameters were input accordingly. The deformation parameters were namely depth, slip, dip angle, strike angle, slip angle, length of the fault, width of the fault and the origin coordinates of the earthquake (Suppasri et al., 2011).

3.2 Analysis of risk

Risk analysis was carried out based on the vulnerability rating and the hazard rating of building structures assigned according to the Disaster Management Centre of Sri Lanka's (DMC) guidance. The hazard rating was assigned depending on the inundation level and the vulnerability rating was assigned based on the susceptibility of the building structures for damage. A survey of 3506 building structures carried out by DMC was utilized for the assessment. Equation 1 was derived in order to

$$R^1 \text{ Hazard} \times \text{Vulnerability} = \text{Risk} \text{ ---- (1)}$$

General building type was further assessed by developing fragility curves with the use of field survey data. Fragility curves were developed to predict the damage probability for a given inundation depth. The damage levels considered for the fragility curve development were minor, moderate, major and complete damage.

4. Results

4.1 Inundation output

The outputs of the tsunami inundation depth calculated from different spatial resolution data types namely ASTER, LiDAR and SRTM are

illustrated in Figure 4.1. The inundation is classified into four main levels to illustrate a comprehensive output on how the inundation varies along the terrain. Results generated with LiDAR data depict an inundation depth of 5-10 m in the areas away (more than 1km) from the coast while an inundation depth of 10 - 17m was observed in the areas nearby (less than 1km) the coast line.

4.2 Risk Assessment

By multiplying the hazard rating and the vulnerability rating the risk assessment was conducted. Four indices 1, 4, 7 and 10 were assigned to the hazard rating based on the modelled inundation maps. Hazard index 1 represents lowest inundation whereas hazard index 10 represents highest inundation. Vulnerability indices 1, 5 and 10 were assigned to single story reinforced concrete buildings (type 1), multiple story reinforced concrete buildings (type 2) and general buildings (type 3) respectively.

The calculated risk index is a value varying from 1 to 100 (where 1 indicates the lowest risk and 100 indicates the highest risk) assessed on 3 types of buildings. The results were segregated according to the initial datasets with different spatial resolutions (i.e. LiDAR, ASTER and SRTM). From the initial datasets, 9 outputs were obtained, i.e. 3 from each dataset with different building construction type (type 1, 2 and 3). Risk mapping for building type 1, 2 and 3 are illustrated in figures 4.2, 4.3 and 4.4 respectively.

All SRTM outputs fall very close to LiDAR outputs. In addition to the remote sensing approach, field data was utilized in this study to develop fragility curves. The fragility curves were developed for the general building structures (Figure 4.5). It was assumed that most of the people with a low economic background occupied the type 3 building structures. Additionally, verification for the outputs from the remote sensing approach was provided by the developed fragility curves. The tabulated results in Table 4.1 illustrate the maximum inundation required to cause 100% damage of the respective damage levels.

Table 4.1: Verification of test results

Damage level	Fragility curve reference (m)	LiDAR output (m)	SRTM output (m)	ASTER output (m)
Minor	6.1	2	1	3
Moderate	7.06	5	5	6
Major	9.17	9	10	11
Complete	10.6	13	15	16

5. Discussion

The correlation values were calculated against the measured inundation depths of 2004 tsunami in Hambantota (documented in Wijetunge, 2008) and the study outputs conducted using the remote sensing approach. 0.8901, 0.8226 and 0.8801 were the correlation values for LiDAR, ASTER and SRTM datasets respectively. The correlation indices suggested that modelled outputs from LiDAR dataset stands very close

to the measured inundation values. Modelled SRTM outputs were impressively close to the measured inundation values. With further available measured depths the correlation index can be enhanced. During the tsunami simulation process the "roughness" was assumed to be a constant value. But in reality, the roughness values vary along the terrain. Thus, different zones with different roughness levels have to be identified through field surveys in order to perform a comprehensive risk assessment.

In the fragility curve analysis, to cause complete damage (Probability =1) to type 3 building the inundation depth was calculated to be 10.6 m. A 13 m inundation depth was observed from the LiDAR dataset to cause heavy damage utilizing the remote sensing approach (LiDAR outputs). 15 m and 16 m inundation depths were observed from the SRTM and ASTER outputs respectively. A close relationship between the fragility curves outputs and the modelled risk outputs was observed thereby the verification was successful. ASTER results were proved to deviate a lot from the measured inundation values. DEMs developed from optical sources such as ASTER can be negatively impacted by the frequency of the cloud cover whereas SRTM penetrates clouds quite easily (Chirico, 2004).

Sand dunes and forestation along the coast line will reduce the energy of a tsunami wave. Rock barriers will also serve the purpose of the energy reduction of the waves. Reinforced concrete structures can be encouraged to reduce the risks as the study presented low risk levels for them. The areas for the general building types can be demarcated to enhance safety of both human lives and property. Based on the study results areas can be demarcated for a specific building type. The risk maps generated in this study will be beneficial in understanding how the risk is diffused over the terrain. The maps will facilitate the decision makers to prepare evacuation plans. Awareness sessions and public education can be encouraged in the potential tsunami risk prone areas. Occasional emergencies can be created and the people can be trained on how to act in the case of a tsunami event. The area for rehabilitation can also be determined effectively.

6. Conclusion

The results from input datasets of three different spatial resolutions (i.e. LiDAR,

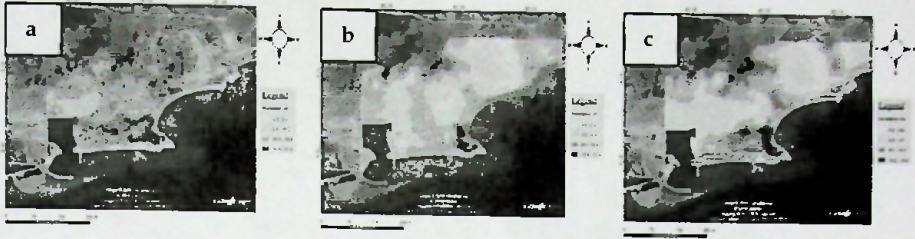


Figure 4.1: Inundation modeled by INSPIRE web portal for 2004 Tsunami parameters using a) ASTER, b) LiDAR and c) SRTM data

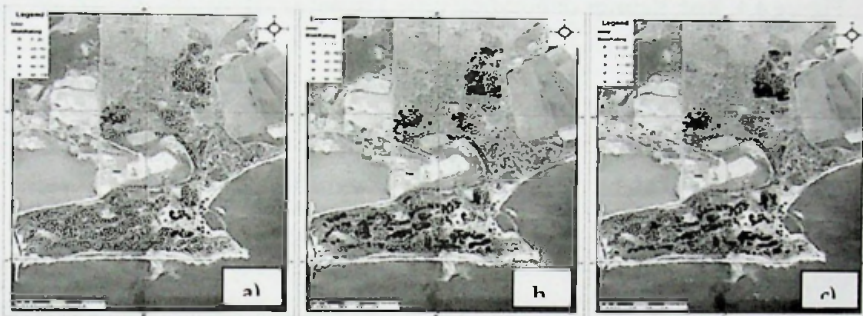


Figure 4.2: Risk Ratings of building type 1 using a) LiDAR, b) ASTER and c) SRTM



Figure 4.3: Risk Ratings of building type 2 using a) LiDAR, b) ASTER and c)

SRTM and ASTER) were analyzed and found that SRTM outputs stand closely to the LiDAR outputs, although SRTM has lower spatial resolution than ASTER. The aforementioned phenomenon was true for both inundation and the risk assessment phases. LiDAR data is considered to be very expensive. Hence hazard and risk analysis

through SRTM data will provide an ideal and economical platform for preliminary risk assessment.

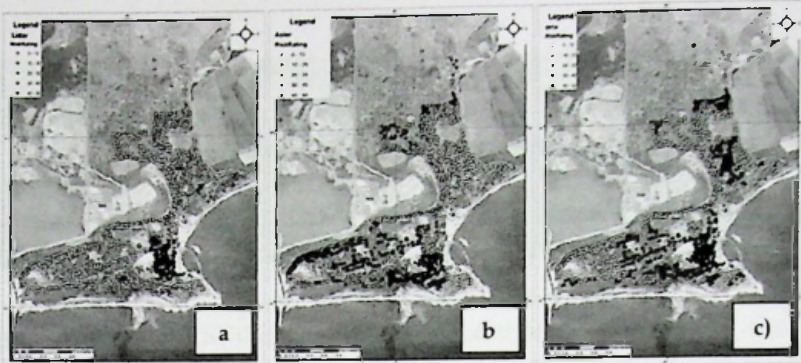


Figure 4.4: Risk Ratings of building type 3 using a) LiDAR, b) ASTER and c) SRTM

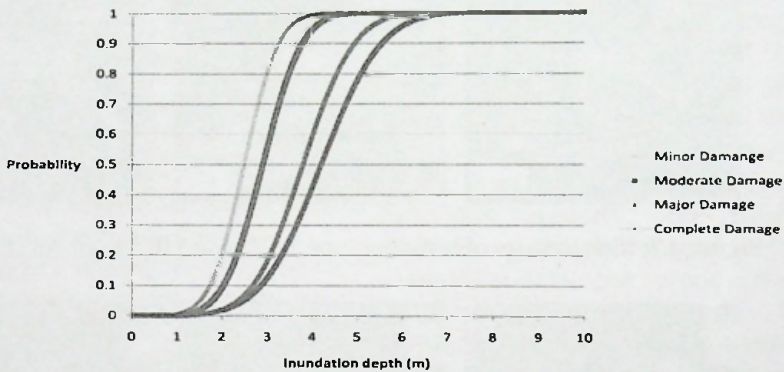


Figure 4.5: Developed fragility curves for type 3 building structures in Hambantota, Sri Lanka

Remote sensing and GIS approach will pave the way to a time and cost saving analysis in an immediate action required environment. The methodology can also be adopted, in modelling the tsunami risks in other potentially tsunami threatened areas in the island such as Batticaloa, Matara, Galle, Ampara etc. and consequently provide a framework to mitigate the devastation that can be caused by a tsunami.

Acknowledgement

Authors wish to thank DMC, Sri Lanka for providing data and access to the INSPIRE web portal.

References

- Berger, E. (2010). Ten Deadliest Natural Disasters since 1900. Retrieved February 10, 2015, from <http://blog.chron.com/sciguy/2010/0>

1/ten-deadliest-natural-disasters-since-1900/

- Bryant, E. (2014). *The Underrated Hazard, Tsunami*, Springer, Third edition.
- Chirico, G. P. (2004). LIDAR derived 5 m resolution Bare Earth and First Return Digital Elevation Model of the Paine Run Watershed, Augusta County, Virginia, U.S. Geological Survey Open-File Report 2004-1320.
- Suppasri A, Koshimura S and Immamura F, (2011), Developing tsunami fragility curves based on the satellite remote sensing and the numerical modelling of the 2004 Indian Ocean tsunami in Thailand, 11, 173-189.
- Wijetunge J.J. (2008). Indian Ocean Tsunami on 26 December 2004: Numerical modelling of inundation in three cities on the south coast of Sri Lanka. *Journal of Earthquake and tsunami*, 2 (2), 133-155.